Journals Pub

International Journal of
Composite Materials and Matrices

ISSN: 2582-435X
Volume 10, Issue 2, 2024
DOI (Journal): 10.37628/IJCMM

https://journals.stmjournals.com/ijcmm/

Research ijcmm

Three Dimensional (3D) Structure and Morphology of Carbon Fibers from X-Ray Microscopy (XRM) Analysis†

†*Dedicated to the legendary polymer chemist Professor Xinling Wang, SJTU, Shanghai, for introducing interface characterization techniques.*

Indra Neel Pulidindi[1*]

Abstract

X-ray microscopy is an elegant chemical imaging technique that bridges the gap between light microscopy and electron microscopy. Vital information on the chemical state (valency, surface functionality), chemical composition, three-dimensional (3D) chemical structure (order, disorder, rupture), and chemical imaging can be obtained from X-ray microscopy. In the current original research article, X-ray microscopy is used as a characterization tool to examine the microstructural features of commercial carbon fibers. Pitch-based (NX100) and polyacrylonitrile (PAN)-based (T700SC) CFs chosen as representative examples for the two major classes of CF feedstock were examined using XRM. A homemade and simple sample preparation technique was developed by gluing the single filament of the carbon fiber (3 mm height) to the flat end of the office pin, which was subsequently held vertically above the XRM sample holder. The XRM imaging instrument was operated at a voltage of 50 kV and at a power of 4.0 W all through the 3D structural characterization of the carbon fibres. Cross-sectional imaging of the carbon fibers (NX100) showed core shell type structure with a clear contrast in the X-ray absorption in the outer and the inner regions of the fiber. From the outer region to the inner region of the fiber (though the structure remained the same), the density of the graphitic structure increased significantly. The core of the pitch-based fibers is highly crystalline compared to the PAN-based fibers. This observation provided additional support for the conclusions drawn from the CFs' XRD and Raman analyses. The 3D microstructural images of the cross-section of the CFs were constructed using TXM3DVIEWER software. In addition, the 3D microstructure of the whole of the single filament of CFs was constructed with the same software. The difference in the 3D microstructure of the NX100 and T700SC is due to the difference in the feedstock as well as the processing conditions. The microstructure of the CFs deduced from XRM is discussed in detail in comparison with the scanning transmission X-ray microscope images of the pitch-based (YSH50H) and PAN-based (M46J) carbon fibers reported in literature. Analogous to the present XRM investigation, the state-of-the-art STXRM studies also showed that the raw material had a considerable impact on the distribution of the π-orbital-orientated domains in the CF structure.

***Author for Correspondence**
Indra Neel Pulidindi
E-mail: indraneelp@jesusconsultancy.com

[1]Jesus' Scientific Consultancy for Industrial and Academic Research (JSCIAR), Tharamani 600113, Chennai, Tamilnadu, India.

Received Date: October 22, 2024
Accepted Date: October 27, 2024
Published Date: December 02, 2024

Citation: Indra Neel Pulidindi. Three Dimensional (3D) Structure and Morphology of Carbon Fibers from X-Ray Microscopy (XRM) Analysis. International Journal of Composite Materials and Matrices 2024; 10(2): 23–32p.

Keywords: XRM, X-ray microscopy, scanning transmission X-ray microscopy, STXRM, carbon fibres, NX100, T700SC, 3D microstructure, XRM imaging, morphology, ZEISS Xradia520versa

INTRODUCTION

The XRM technique provides quantitative, high resolution, three-dimensional, microstructural information on carbon fiber reinforced plastics (CFRPs) in general and carbon fibers (CFs) in particular. The non-destructive nature of the X-rays helps examining the structural changes in composites before and after the application of

tension or shear, leading to knowledge on the changes that took place in the composite material. In addition, vital information on the interface of CFRPs can be deduced from XRM analysis [1]. X-ray microscopies bridge the gap between the conventional electron and light microscopies and are useful for the imaging of extremely large as well as complex structures. Local chemical composition, chemical state (valency, surface chemical functionality), and microstructure can be viewed with good spacial resolution [2]. Unlike the electron beams, X-rays are soft and form a potential chemical imaging technique with good spatial resolution at the nanoscale for the analysis of organic compounds as well [3]. Though a Google search with the keyword, namely, X-ray microscopy, yields 47, 70, 000 results, the number reduces by two orders of magnitude (16,300) when the keywords, namely, X-ray microscopy and CFRPs, are crossed together. This testifies to the very fact that though the X-ray microscopy (XRM) technique is very informative to gain both qualitative and quantitative insights into the 3-dimensional (3D) structure (micro and nano) and morphology of exotic and advanced materials like carbon fiber reinforced plastics (CFRPs), the technique is not explored yet to its fullest [4–16]. Scientific literature is very scarce on the use of XRM as a characterization tool for probing the micro and nano 3D architecture (structure and morphology) of advanced chemical and biological materials. The same thing is true for another vital nanoprobe, namely, atomic force microscopy (AFM), a potential interface characterization technique. Crossing the keywords, namely, atomic force microscopy and CFRPs, yields only 9790 results. [17–22].

The current research article deals with the systematic characterization of the 3D microstructure of the commercial-sized carbon fibers, both pitch-based (NX100) and polyacrylonitrile-based (T700SC), and comparing the results obtained with the classical structural analytical tools, namely, the XRD, Raman, and scanning transmission X-ray microscopy (STXRM).

Experimental

Pitch-based carbon fibers, namely, NX100, were procured from nippon graphite fiber co. Polyacrylonitrile, PAN-derived CFs, namely, T700SC, were purchased from Toray Ltd. 3D structure as well as the structure at the cross-section (internal structural features) of carbon fibers, namely, NX100 (representative example for pitch-based carbon fibers) and T700SC (representative example for PAN based carbon fibers), is examined using X-ray microscopy. The image of X-ray microscope (ZEISS Xradia520versa, Voltage: 50 kV, Power: 4.0 W) used for the study and the location of the sample holder (with the single filament of carbon fiber of length ~3 mm glued to the holder) between the X-ray source and the detector is shown in Figure 1.

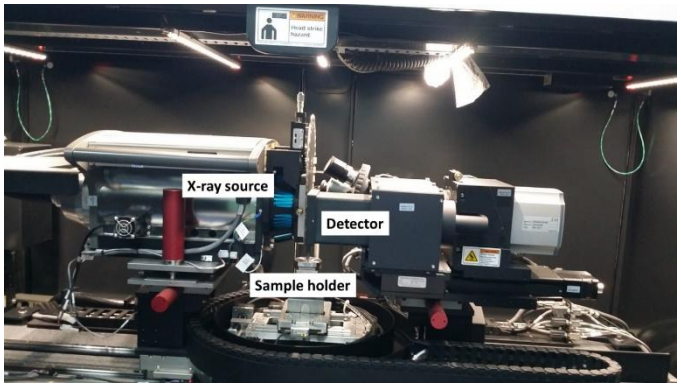

Figure 1. X-ray microscope instrument used for the analysis of the three-dimensional (3D) structure of carbon fibers X-ray microscope (ZEISS Xradia520versa, Voltage: 50 kV, Power: 4.0 W).

The sample preparation as well as the analysis of the 3D as well as the internal structure by X-ray microscopy is a time-consuming process, unlike simple XRD analysis. The carbon fiber sample preparation for XRM analysis consists of gluing a single filament of carbon fiber (NX100 and T700SC) to the office pin (the flat end of the pin is cut off, and only the pin without the flat end is used in the sample preparation). The office pin with the single filament of carbon fiber glued to it was mounted in

the sample holder. With scissors, the fiber length is adjusted to nearly 3 mm, cutting off the rest of the length of the fiber. The sample holder upon which the office pin is glued with the single filament of carbon fiber is shown in Figure 2. As the diameter of the fiber NX100 is only 12 μm, it is not visible to the naked eye in the image shown. Only the tip of the office pin is seen, and at the tip the invisible single filament of carbon fiber (NX100) of length 3 mm is present glued to the top of the office pin.

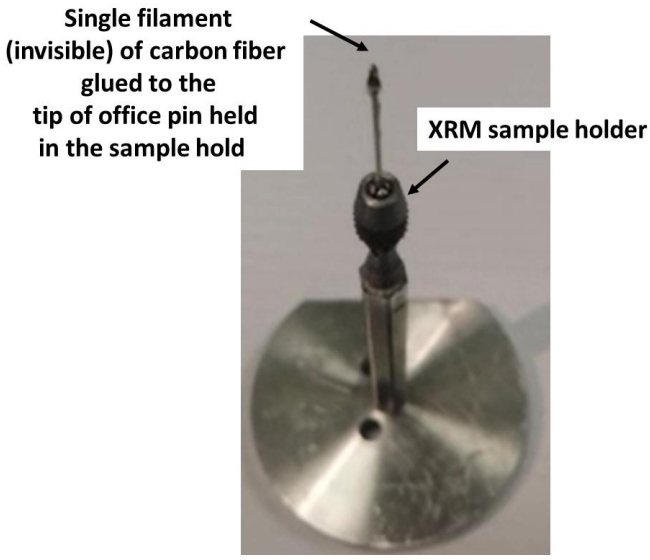

Figure 2. XRM sample holder holding the office pin on to which the single filament of carbon fiber of length ~3 mm is glued.

RESULTS AND DISCUSSION

3D Structure of Carbon Fibers Using X-Ray Microscopy (XRM)

The XRM image of the cross section of the carbon fiber NX100 reveals the internal structure of the carbon fiber at the cross section, as shown in Figure 3. Throughout the XRM analysis, the instrument (ZEISS Xradia520versa) is operated at a voltage of 50 kV and at a power of 4.0 W. What is to be noticed in the XRM image of NX100 depicting the structure of the cross-section is the contrast of the brightness (Figure 3). The diameter of the carbon fiber NX100 of 12.6 μm is marked in the image of the cross section. Outside and around the circumference of the carbon fiber there is some unusual dark region spreading over nearly ~2.7 μm and the origin of such shadow around the carbon fiber is unclear and could be attributed to the conditions of analysis and mode of operation of the XRM machine. Such shadowing effect is more a technical issue rather than an issue of chemical significance pertaining to the structure of the carbon fiber and so can be neglected, as far as the discussion on the structure of the carbon fiber is concerned. At the shell the brightness is higher and as we go into the core the brightness is diminished, and gray regions are observed. This contrast in brightness indicates that the cross section of the carbon fiber comprises of an amorphous shell (bright region) and a crystalline core (grey regions). Such core-shall structure of carbon fiber is of immense use as far as interfacial shear strength of carbon fiber is concerned. Such structure facilitates transfer of stress from the shell to the core, in the load bearing component, namely, the carbon fiber, of the carbon fiber reinforced composite. Two black dark spot like features are visible in the cross section of the carbon fiber NX100. These two dark black spots are attributed to highly graphitic regions in the internal structure of the carbon fibers. The formation of such high density graphitic chemical structures could be due to the existence of concentric multiwall carbon micro-tube like structures in the core of the fibers. The vital question that arises then is that why at all such micro-graphitic tubes of carbon should prevent the passage of X-rays from the source to the detector making a black spot. Imagine a set of concentric graphitic tubes with wide pore mouth narrowing down along the length (like concentric cones) and fusing down together at the other end of the tube. Such a situation prevents the passage of X-rays from the source to the detector. In fact, the XRD and Raman analysis, that examines the bulk structure of the carbon fibers showed features like

multi walled carbon nanotubes in the highly graphitic structure of carbon fibers, predominantly in pitch-based fibers (NX90 and NX100) [23, 24]. However, caution should be exercised in drawing conclusion as to the nature of such dark black spots in the structure of cross section of carbon fibers (Figure 3). More scientific literature on XRM analysis to be consulted and further experimentation of the pitch-based fibers by XRM should be taken up before drawing conclusions on the nature of the dark spots as those seen in Figure 3. In fact, existence of macro pore network structure in PAN-based carbon fibers are reported [25].

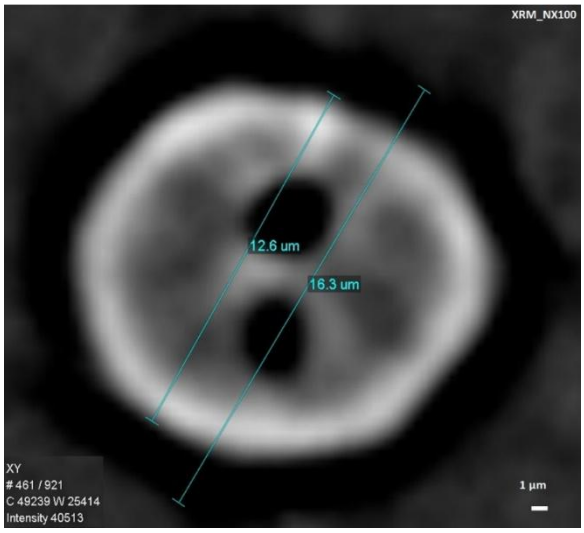

Figure 3. Core-shell structure of the cross-section of the single filament of carbon fiber NX100 derived from the 3D structure generated from X-ray microscope analysis.

For comparison, the region of the cross section of the carbon fiber (NX100) examined by the XRM and the resulting structure of the cross section, the internal structure of the whole carbon fiber, and the 3D image of the cross section constructed using TXM3DVIEWER were shown in Figure 4. The 3D image of the cross section constructed using TXM3DVIEWER (enlarged version) as well as the 3D structure of the whole single filament of NX100 constructed using TXM3DVIEWER are shown in Figure 5.

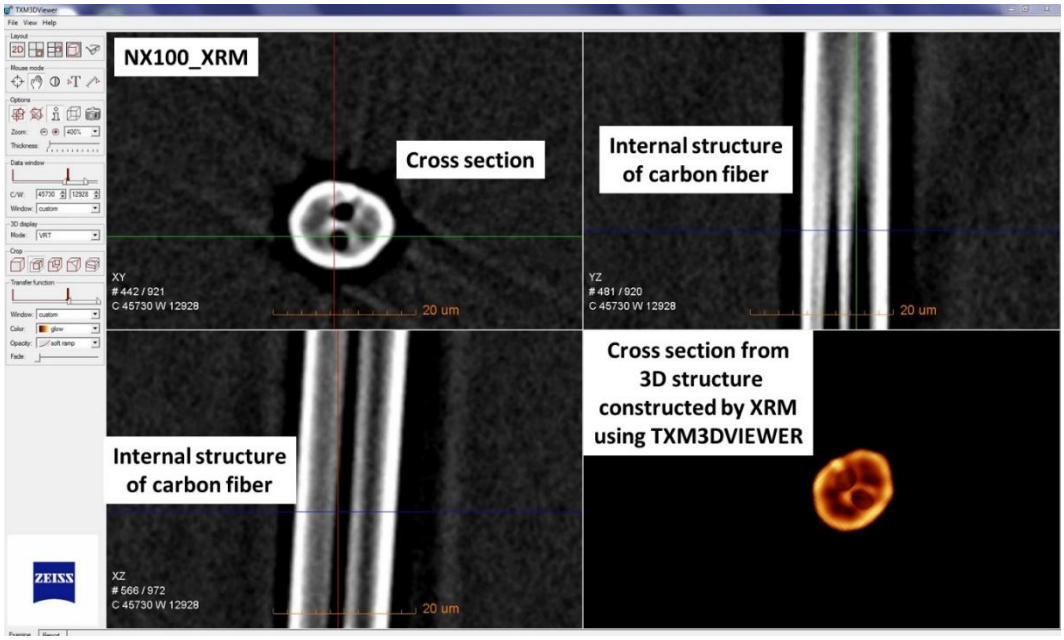

Figure 4. Cross section, the internal structure of the single filament of carbon fiber NX100

and the image of the cross section derived from the 3D structure constructed from X-ray microscope analysis using TXM3DVIEWER.

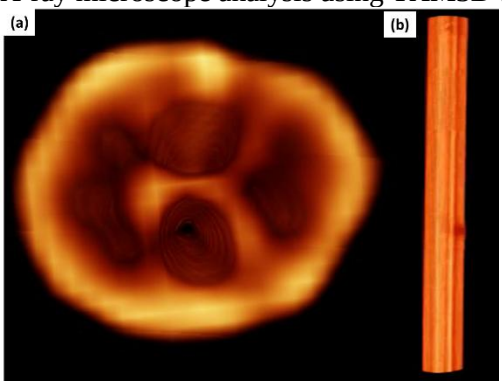

Figure 5. View of (a) cross section and the (b) 3D structure of the single filament of carbon fiber NX100 constructed from the 3D structure generated from X-ray microscope analysis using TXM3DVIEWER.

The XRM image of the cross section of the carbon fiber T700SC (PAN-based), revealing the internal structural features of the carbon fiber, is shown in Figure 6. Analogous to the XRM image of the cross section of the pitch-based carbon fibers NX100, the structure of T700SC also consists of the shell, which is made up of highly disordered layers of graphene, and the core, which is a relatively ordered and more crystalline graphitic carbon structure. Such structural features are understood from the contrast of brightness seen in the XRM image. As we go from the shell to the core, the brightness decreases and gray region is observed at the core. The gray region means hindrance to the passage to X-rays from the source to the detector. Such hindrance is by the well-ordered graphene sheets at the core. The revelations from XRM are consistent with the XRD and Raman findings that pitch-based fibers are more crystalline than PAN-based fibers [23, 24]. Additional knowledge that can be gained from XRM beyond the XRD analysis is that the amorphous and crystalline regions in the carbon fiber structure are clearly seen. There is still scope for improvement in resolution of the images of XRM, and further attempts should be devoted in that direction to obtain more insights into the internal and 3D structure of carbon fiber by improving the resolution. The diameter of the carbon fiber T700SC is ~7.1 μm, as marked in Figure 6. The striking contrast between the structure of cross section of NX100 (Figure 3) and the structure of the cross section of T700SC is that the dark black spots (highly crystalline regions) present in NX100 are absent in T700SC. Again, such a difference is anticipated as the source of raw materials of these two carbon fibers itself is different [23, 24]. For comparison, the region of the cross section of the carbon fiber (T700SC) examined by the XRM and the resulting structure of the cross section, the internal structure of the whole carbon fiber, and the 3D image of the cross section constructed using TXM3DVIEWER are shown in Figure 7. The 3D image of the cross section constructed using TXM3DVIEWER (enlarged version) as well as the 3D structure of the whole single filament of T700SC constructed using TXM3DVIEWER were shown in Figure 8.

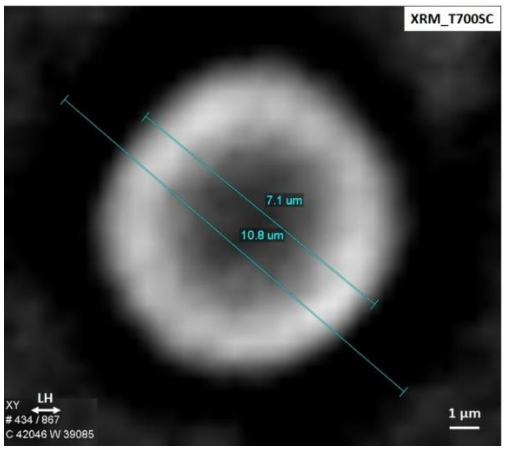

Figure 6. Core-shell structure of the cross-section of the single filament of carbon fiber T700SC (PAN-based), derived from the 3D structure generated from X-ray microscope analysis.

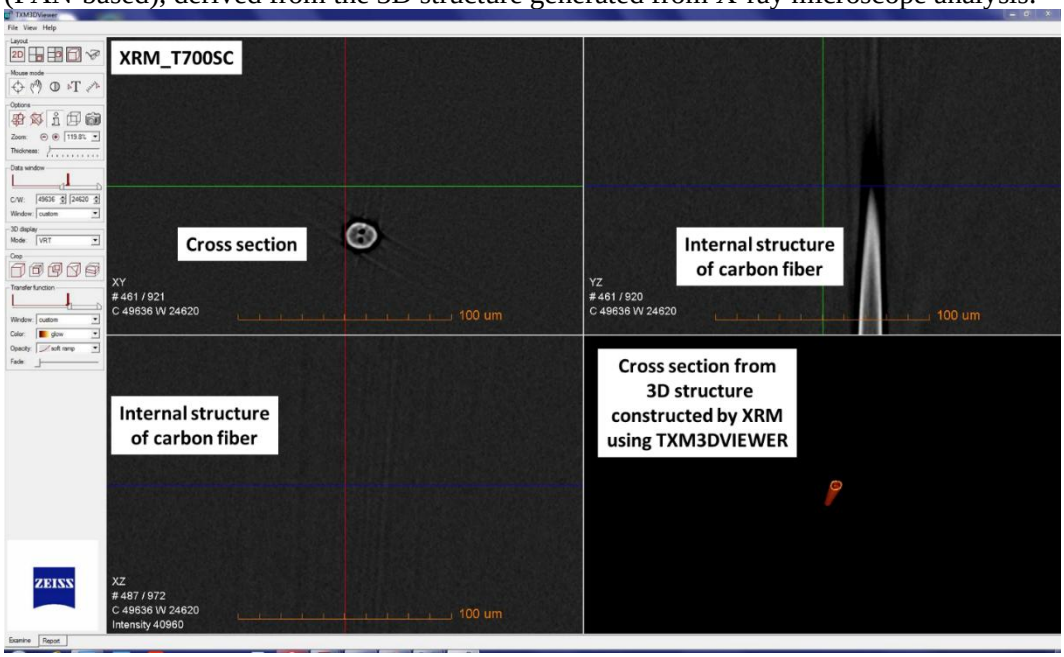

Figure 7. Cross section, the internal structure of the single filament of carbon fiber T700SC and the image of the cross section derived from the 3D structure constructed from X-ray microscope analysis using TXM3DVIEWER.

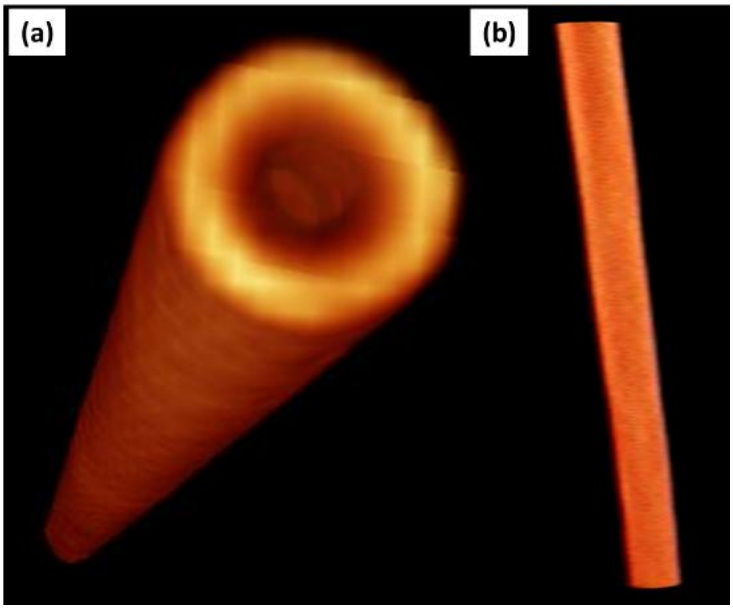

Figure 8. View of (a) cross section and the (b) 3D structure of the single filament of carbon fiber T700SC constructed from the 3D structure generated from X-ray microscope analysis using TXM3DVIEWER.

A comparison of the structure of cross sections of pitch and PAN-based fibers is provided in Figure 9. The dark ring-shaped shadow around the fiber circumference can be neglected for discussion as this has nothing to do with the structure of the carbon fiber. Irrespective of the source of the carbon fiber, the shell of the CFs is bright, and the core is gray. Such a contrast reflects that the shell is made up of amorphous graphitic crystallites while the core is made up of crystalline graphitic crystallites. The core of the NX100 is dark gray, while that of the T700SC is light gray. The darker the gray core, the greater

the crystallinity. Thus, pitch-based fibers (NX100) are more crystalline compared to PAN (T7007C) based fibers (Figure 9).

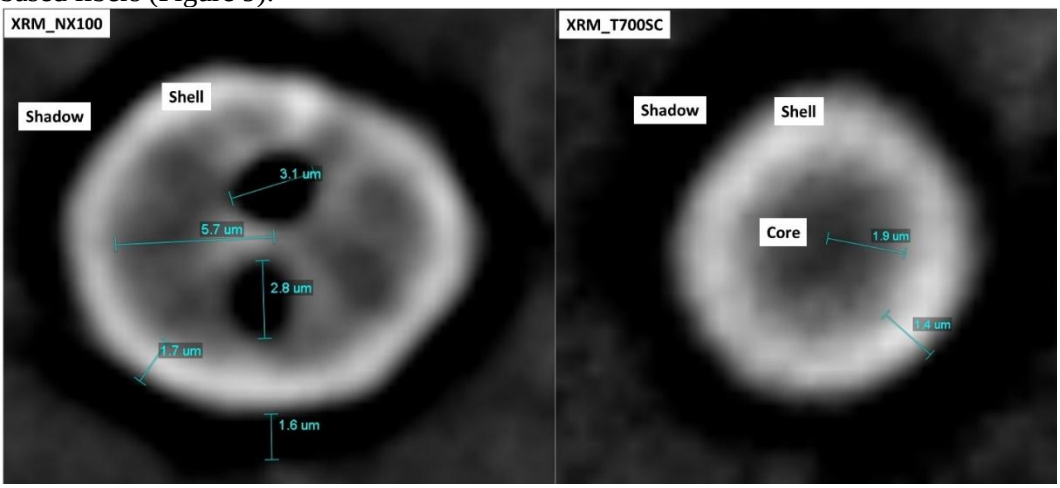

Figure 9. Structure at the cross section of carbon fibers NX100 and T700SC – a comparison.

A specific case of the appearance of a void (dark spherical region) in the cross-sectional image of twintex composite is reported [1]. An XRM image of the sample of twintex composite comprising of a four-layer thermoplastic (85 x 17 x 2 mm) was recorded at 1 μm voxel at 40 kV. E-glass and polypropylene fiber reinforcements are incorporated into a continuous fiber composite, which is composed of a polymer matrix. The polypropylene fibers (dark), E-glass fibers (bright), and voids (dark spherical regions) are clearly seen in the cross-sectional structure of the composite. Likewise, in the 3D internal structure of the composite, the E-glass fibers (green), polypropylene fibers (orange), and voids (white spheres) were observed distinctly differently [1].

For comparison, the TEM and scanning transmission X-ray microscopy (STXRM) images of PAN-based (M46J) and pitch-based (YSH50H) carbon fibers were shown in Figure 10 [26].

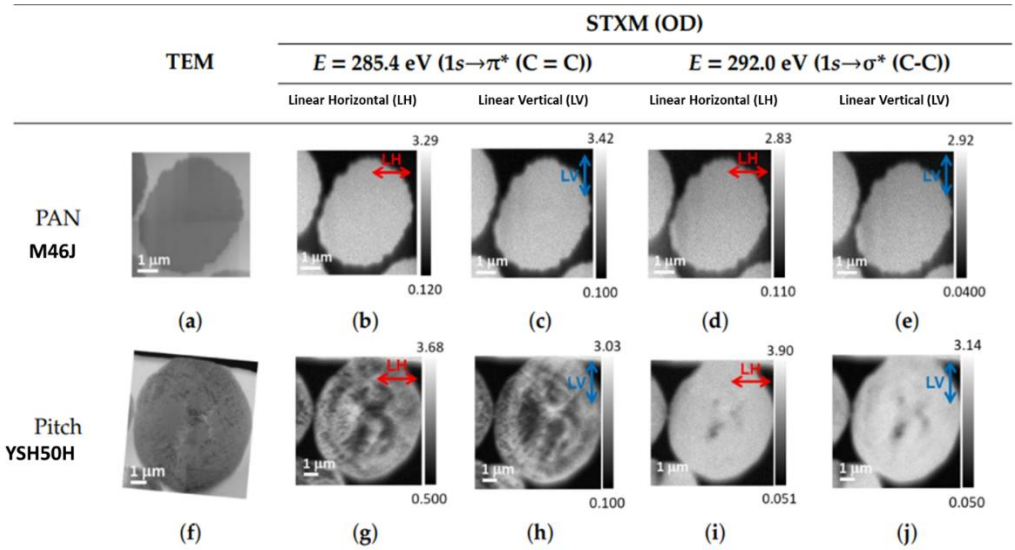

Figure 10. (a) and (f) TEM (bright field) images of the cross section of the PAN (M46J) and pitch (YSH50H) based CFs, respectively; (b–e), (g–j) optical density (OD) images obtained using scanning transmission X-ray microscopy (STXRM) at the energies 285.4 eV (1s → π*) and 292 eV (1s → σ*) with linear horizontal (LH) and linear vertical (LV) polarized beams. "f" is rotated to align with the X-ray absorption images (g–j) [26].

To evaluate the micro-texture of carbon fibers that play a crucial role in controlling the physical properties, namely, tensile strength and tensile modulus, STXRM studies were carried out on both pitch and PAN-based carbon fibers. Regions where the π-orbitals in each graphite crystallite align in the same direction to the degree that Bragg's law is not satisfied are known as π-orbital-oriented domains. Conversely, the stacks of graphene sheets within a single graphite crystallite are known as stacked structures of graphene sheets [26]. Figure 10 displays the TEM and X-ray absorption pictures of the PAN and pitch-based CFs' cross sections taken with STXRM

at energies of 285.4 eV (1s → π*) and 292 eV (1s → σ*). It was observed that in the case of PAN-based fibers, the contrast (optical density, OD) in the X-ray absorption images at 285.4 eV (images b and c) and at 292.0 eV (images d and e) was independent of the direction of the X-ray polarization. The red and blue arrows in Figure 10 correspond to the X-ray polarization direction (LH-linear horizontal; LV-linear vertical). It is discovered that the π-orbital domain sizes in the PAN-based CFs' cross section are less than the 50 nm spatial resolution of STXM (Figure 10(b–c)). In contrast to the response of PAN-based fibers, the OD pictures of pitch-based CFs at E = 285.4 eV (Figure 10(g–h)) showed X-ray absorption as a function of polarization direction. There is an opposing contrast between the polarization of the LH and LV. However, when the OD images were recorded at E = 292.0 eV, no dependence of OD on the direction of X-ray polarization was noticed (Figure 10(d–e)). This is because of the symmetry of the σ orbital that showed no dependence of OD on the direction of polarization. The pitch-based fibers were made up of π-orbital-oriented domains that were larger than the resolution of STXRM, or 50 nm, and ranged in size from about 100 to 1000 nm (Figure 10(g–h)). Thus, the carbon fiber structure is mapped using STXRM and two orthogonal linearly polarized X-rays, providing information on the longitudinal and cross sections of PAN and pitch-based CFs. The distribution of π-orbital directed domains in the carbon fiber structure differed significantly depending on whether PAN or pitch was utilized as the raw material for the carbon fiber manufacturing. Conversely, there is no discernible difference between the PAN and pitch-based CFs in terms of the distribution of the σ-orbital orientations. PAN-based CFs had a cross section made up of randomly distributed π orbital domains that were smaller than about 50 nm in size, whereas pitch-based CFs had a cross section made up of π-orbital-oriented domains that ranged from 100 to 1000 nm. With breakthroughs in surface modification, especially through sizing, in CFs, the applications of CFs for forming strong interfaces with the polymer matrices leading to functional CFRPs are realized [27–30]. This necessitates the imaging of the interface of CFRPs with soft and non-distructive techniques like XRM.

CONCLUSIONS

Characterizing the chemical state, microstructure, and imaging of carbon fibers in general and the interface of carbon fiber-reinforced plastics, in particular is becoming more and more important as new raw materials, such as lignin and polyethylene replace traditional mesopitch (natural and synthetic) and carbon fibers based on polyacrylonitrile (PAN). X-ray microscopy is reported as a promising chemical imaging and characterization (qualitative and quantitative) technique for the analysis of three dimentional (3D) microstructures of the carbon fibers. The findings from X-ray microscopy imaging strengthened the inferences from the XRD and Raman analysis of carbon fibers, making faith become sight.

Acknowledgments

Indebtedness is due to Professor Xinling Wang, SJTU, for the calm and conducive research environment where the experimental and writing skills of INP blossomed. Thankfulness is due to Dr. Dandan Zhu for the meticulous guidance and steadfast support. Thanks are due to Dr. Chongchong Yang for the timely help and guidance in designing and conducting the experiments. Thanks are due to Professor Zhen Zheng for the fruitful discussion. Grateful thanks are due to Dr. Dechao Meng for assistance in the XRM analysis. Thankfulness is due to the true physicist, Dr. Trupti Gajaria, GSFCU, for the constant motivation. Indebtedness is due to the beloved brothers and sisters of the Minhang Evangelical Church, Minhang, Shanghai, for the fellowship and love.

REFERENCES

1. Xraida. X-ray microscopy analysis (XRM) of fiber-reinforced composite materials [Online]. AZO Material. 2013, April 22. Available from: https://www.azom.com/article.aspx?ArticleID=8530#:~:text=X%2Dray%20microscopy%20(XRM)%20offers%20quantitative%2C%20three%2D,to%20observe%20micro%2Dstructural%20changes.
2. Sayre D, Chapman HN. X-ray microscopy. Acta Cryst. 1995;A51:237–252. doi:10.1107/S0108767394011803.
3. Harano T, Murao R, Takeichi Y, Kimura M, Takahashi Y. Observation of the interface between resin and carbon fiber by scanning transmission X-ray microscopy. J Phys Conf Ser. 2017;849:012023. doi:10.1088/1742-6596/849/1/012023.
4. Jacobsen C. X-ray Microscopy: Advances in Microscopy and Microanalysis. Cambridge, UK: Cambridge University Press; 2020.
5. Falcone R, Jacobsen C, Kirz J, Marchesini S, Shapiro D, Spence J. New directions in X-ray microscopy. Contemp Phys. 2011;52(4):293–318. doi:10.1080/00107514.2011.589662.
6. Cosslett VE, Nixon WC, X-ray Microscopy. Cambridge, UK: Cambridge University Press; 1960.
7. Vogtmann J, Klingler A, Rief T, Gurka M. 3D X-ray microscopy as a tool for in depth analysis of the interfacial interaction between a single carbon fiber and an epoxy matrix after mechanical loading. J Compos Sci. 2021;5(5):121. doi:10.3390/jcs5050121.
8. Kimura M, Watanabe T, Oshima S, Takeichi Y, Niwa Y, Kitazawa R, et al. Nano-to macroscale In Situ observation of microcrack formation in carbon fiber-reinforced plastic under loading using synchrotron transmission X-ray microscopy. AIP Conf Proc. 2023;2990(1):020008. doi:10.1063/5.0169168.
9. Pournoori N, Soares GC, Lukić B, Isakov M, Belone MCL, Hokka M, et al. In situ damage characterization of CFRP under compression using high-speed optical, infrared and synchrotron X-ray phase-contrast imaging. Compos Part A Appl Sci Manuf. 2023;175:107766. doi:10.1016/j.compositesa.2023.107766.
10. Kimura M, Obayashi I, Kido D, Niwa Y, Gao X, Akagi K. Finding “Trigger Sites” of Reactions Among Heterogeneous Materials from X-ray Microscopic Big Data Using Persistent Homology. In TMS Annual Meeting & Exhibition Supplemental Proceedings. TMS 2024. The Minerals, Metals & Materials Series. Cham, Switzerland: Springer; 2024. 784–792. doi:10.1007/978-3-031-50349-8_67.
11. Yamane H, Oura M, Yamazaki N, Ishihara T, Hasegawa K, Ishikawa T, et al. Visualizing interface-specific chemical bonds in adhesive bonding of carbon fiber structural composites using soft X-ray microscopy. Sci Rep. 2022;12(1):16332. doi:10.1038/s41598-022-20233-4.
12. Takahashi K, Shoya R, Matsuo T, Sato W, Nakamura T, Takeuchi A, et al. X-ray nanoimaging of a transversely embedded carbon fiber in epoxy matrix under static and cyclic loads. Sci Rep. 2022;12(1):8843. doi:10.1038/s41598-022-12724-1.
13. Lu T, Chen X, Wang H, Zhang L, Zhou Y. Comparison of low-velocity impact damage in thermoplastic and thermoset composites by non-destructive three-dimensional X-ray microscope. Polym Test. 2020;91:106730. doi:10.1016/j.polymertesting.2020.106730.
14. Rosemeier M, Lester C, Antoniou A, Fahrenson C, Manousides N, Balzani C. Determination of as-built properties of fiber reinforced polymers in a wind turbine blade using scanning electron and high-resolution X-ray microscopy. Compos Part C Open Access. 2022;9:100310. doi:10.1016/j.jcomc.2022.100310.
15. Staab F, Prescher M, Balle F, Kirste L. 3D X-ray microscopy of ultrasonically welded aluminum/fiber-reinforced polymer hybrid joints. Mater. 2021;14(7):1784. doi:10.3390/ma14071784.
16. Kimura M, Takeichi Y, Watanabe T, Niwa Y, Kimijima KI. Finding degradation trigger sites of structural materials for airplanes using X-Ray microscopy. Chem Record. 2019;19(7):1462–1468. doi:10.1002/tcr.201800203.

17. Wang A, Li S, Zhang S, Zhang S, Liu Z, Yan K. Enhancing CFRP laminates with plasma jet arrays: A study of interlaminar mechanical properties. Polym Compos. 2024;45(11):10190–10203. doi:10.1002/pc.28466.
18. de Oliveira MM, Runqvist L, Poot T, Uvdal K, Carastan DJ, Selegård L. Hybrid nanofiller-enhanced carbon fiber-reinforced polymer composites (CFRP) for lightning strike protection (LSP). ACS Omega. 2024;9(33):35567–35578. doi:10.1021/acsomega.4c03272.
19. Yang C, Zhu D, Yang F, Liu Q, Sun C, Lei K, et al. Quantitative analysis based on atomic force microscopy characterization of interfacial properties between carbon fibers and epoxy resin subjected to hygrothermal and thermal treatments. Compos Sci Technol. 2020;198:108278. doi:10.1016/j.compscitech.2020.108278.
20. Raimondo M, Naddeo C, Vertuccio L, Lafdi K, Sorrentino A, Guadagno L. Carbon-based aeronautical epoxy nanocomposites: effectiveness of atomic force microscopy (AFM) in investigating the dispersion of different carbonaceous nanoparticles. Polym. 2019;11(5):832. doi:10.3390/polym11050832.
21. Fard MY. Carbon nanotube network and interphase in buckypaper nanocomposites using atomic force microscopy. Int J Mech Sci. 2021;212:106811. doi:10.1016/j.ijmecsci.2021.106811.
22. Liu L, Jia C, He J, Zhao F, Fan D, Xing L, et al. Interfacial characterization, control and modification of carbon fiber reinforced polymer composites. Compos Sci Technol. 2015;121:56–72. doi:10.1016/j.compscitech.2015.08.002.
23. Pulidindi IN. Crystallinity of commercial carbon fibers from X-ray diffraction (XRD) studies. Int J Photochem Photochem Res. 2023;1(1):17–27.
24. Pulidindi IN. Raman spectroscopy for the determination of relative crystallinity of carbon fibers. Int J crystall Mater. 2024;1(1):30–37.
25. Cheng A, Zhang Y, Zhong WH, Li ZP, Cheng DJ, Lin YX, et al. Few layer MoS2 embedded in N-doped carbon fibers with interconnected macro pores for ultrafast sodium storage. Carbon. 2020;168:691–700. doi:10.1016/j.carbon.2020.07.008.
26. Harano T, Takeichi Y, Usui M, Arai Y, Murao R, Negi N, et al. Observation of distribution of π-orbital-oriented domains in PAN- and pitch-based carbon fibers using scanning transmission X-ray microscopy. Appl Sci. 2020;10(14):4836. doi:10.3390/app10144836.
27. Pulidindi IN, Gedanken A. Surface modification of carbon fibers. Preprints. 2023. doi:10.20944/preprints202308.2053.v1.
28. Patel D, Joshi M, Joshi Y, Pulidindi IN, Selvaraj S. Direct synthetic routes of MXenes and their application in carbon fiber reinforced plastics (CFRPs) as supplementary sizing layer. Int J Crystall Mater, 2024;1(1):7–13
29. Pulidindi IN. Diglycidyl ether of bisphenol A (DGEBA) based epoxy sizing agent induces surface polarity in carbon fibers. IJCM. 2024.
30. Pulidindi IN. New insight into the composition and structure of sizing agent from NMR spectroscopy. J Photochem Photochem Res. 2024.

